EEG Based Inference of Causal Cortical Network Dynamics in Reward-Based Decision Making

Hristos S. Courellis [*†], David Peterson [‡§], Howard Poizner [‡], Gert Cauwenberghs [*‡], John Iversen [†‡]
Email: {hcourell,dp,hpoizner,gert,jiversen}@ucsd.edu

* Bioengineering Department, University of California - San Diego, La Jolla, CA, USA
† Swartz Center for Computational Neuroscience, University of California - San Diego, La Jolla, CA, USA
‡ Institute for Neural Computation, University of California - San Diego, La Jolla, CA, USA
§ Computational Neurobiology Laboratory, Salk Institute, La Jolla, CA, USA

Abstract— **Experimental investigation and monitoring of reward signaling implicated in addiction and neurological disorders has traditionally been limited to invasive measurement of deep-brain dopamine activity. Here we introduce a systematic methodology and algorithmic pipeline to quantify causal relationships between regions of interest (ROIs) in the cerebral cortex revealing reward-based signaling pathways involved in human decision making using only non-invasive scalp electroencephalography (EEG). The data is processed by extracting epochs around time-locked stimuli of interest and performing independent component analysis (ICA) on individual datasets to remove artifacts and identify cortical sources. The pipeline entails identifying ROI's with the Measure Projection Toolbox (MPT) through clustering of ICs, localizing current sources in these ROIs using Bayesian inference based constrained low resolution electromagnetic tomography (cLORETA), and computing causal relationships between ROI's using the Source Information Flow Toolbox (SIFT). The proposed methodology and pipeline are demonstrated on 64-channel scalp EEG signals recorded from healthy adults performing a reward-based decision making task conducted through a brain computer interface (BCI) framework. In comparison to a standard method for Group-ICA, our pipeline generates far more biologically plausible and consistent causal connections between ROIs.**

Keywords—; Brain-computer interface; Causality; LORETA; Independent component analysis; Electroencephalography

I. INTRODUCTION

Understanding causal relationships in neural activity between regions of the brain responsible for reward-based signaling during decision making is of paramount importance for both research and diagnosis of behavioral disorders such as addiction and neurological disorders such as Parkinson's disease and depression. Traditionally, the experimental study of reward-based conditioning in the brain has been limited to highly invasive monitoring of dopamine signaling pathways, primarily in the basal ganglia[1]. However, dopamine signaling is not limited to sub-cortical regions, and dopaminergic pathways project from the basal ganglia back into the cerebral cortex. Therefore, we expect that the reward-based signaling originating from sub-cortical activity can be inferred from the causal dynamics of cortical network activity as readily available from non-invasive scalp electroencephalography (EEG). Surprisingly, very few studies have explored the use of EEG as a non-invasive alternative to deep brain monitoring of dopamine-related activity, despite its tremendous potential as a brain-computer interface (BCI) biomarker and neurofeedback training (NFT) based treatment for clinical depression, addiction, and neurological conditions related to Parkinson's disease and other movement disorders.

Motivated by evidence suggesting the existence of an active cortical network involved in making decisions based on anticipated reward [2], analysis of causal relationships among brain regions has been previously performed using EEG signals [3].The approach presented in this paper is adapted from [3] (using measure projections instead of the centroids of IC clusters to identify regions of interest [ROIs] – see section IIB, step 4) and applied to the network suggested by Peterson *et al.* [4] in order to quantify causal relationships among brain ROIs associated with the planning phase of reward-based decisions. In the process, two EEG data processing pipelines are developed, the associated algorithms are discussed, and the following open source software (running within Matlab [The Mathworks Inc.] and Octave) is used: EEGLab [5], MobiLab [SCCN-UCSD], BCILab [6], OpenMEEG [7], and their extensions. The output of the two pipelines is compared and a physiological interpretation of the results is discussed.

II. METHODOLOGY

A. Data Collection Procedure

Full cap EEG data were collected from eleven adult college students between the ages of 18-23, performing a reward-based decision making task. The participants were presented with two images on a computer monitor and asked to select the image that would give them more money. The participants were not informed about the value of each image but had to acquire that knowledge via trial and error throughout the session (of about two hours). Detailed description of the task, the participants, and the data collection can be found in Peterson *et al.* [2]

B. Data Processing -Bayesian Inference based Computation of Temporal Activations using cLORETA

The procedure, algorithms, and Open Source Software associated with processing EEG signals to investigate causal relationships among brain ROIs are demonstrated using EEG signals collected during the reward-based decision making task described above and investigating causal relationships among brain ROIs during the decision phase of the task.

1) Artifact Removal; EEGLab: Infomax based Independent Component Analysis (ICA) [8] was performed on the EEG recordings of each participant to identify independent

This work was supported by NSF ENG-1137279 (EFRI M3C)

978-1-4799-7234-0/15/$31.00 ©2015 IEEE

components, which were classified manually as artifact or cortical sources (using a standard dipolarity criterion).

2) Data Epoching; EEGLab: The data were segmented into Event Related Potential (ERP) epochs around image presentation, encompassing a window of 0.1s before to 1.5s after the presentation for both the decision making and non-decision making conditions. The resulting (512) epochs per participant were separated into decision and non-decision epochs and epochs in each category were concatenated across all EEG channels creating a "control" dataset of non-decision epochs and a "decision" dataset of decision epochs for each participant.

3) IC Clustering; EEGLab: In order to identify spatially and functionally contiguous regions of interest, clustering was conducted on the independent components (ICs) from all participants pooled together, using control and decision epoched data from step-2. Functional metrics for the clustering included the power spectrum, scalp map, event related potential (ERP), dipole location, and event related spectral perturbation (ERSP). These metrics were combined in a preclustering matrix whose dimensionality was reduced via Pricipal Component Analysis (PCA) to allow for rapid clustering convergence. Clustering was accomplished with the use of a competitive layer neural network which converged to the outcome after 1000 iterations.

4) Measure Projection; EEGLab-Measure Projection Toolbox [9]: Since locations of cluster centroids do not provide information about the locations of all ICs distributed within clusters, Measure Projection analysis was used to determine regions of interest (ROI's) based on a selected functional metric. Of the metrics used in clustering, ERSP provides the most functional information, giving a spectral decomposition of the ERP along the epoch time window. 3D volumetric domains with consistent ERSP's were projected into a standard cortical volume, and anatomical locations were determined from the voxels contained within each of the 3D domains, and confirmed with the clustering results.

5) Head Model Construction; Mobilab - OpenMEEG: A standardized head model was created for all the participants by transforming the 64 original channel locations to MNI coordinate space and subsequently warping a standard head model (MRI MNI Colin27), contained in MobiLab, such that the individual layers of the head model (i.e. brain, CSF, skull, scalp) matched the shape given by the MNI-warped channels. The Colin27 model is a boundary element model (BEM) with 4825 vertices on which current source localization can occur, and the lead field matrix for the BEM was calculated using OpenMEEG.

6) Source Localization; BCILab: Current sources for each participant were computed at preselected anatomical locations (based on measure projections) using anatomically constrained LORETA [10] (cLORETA)with bayesian hyperparameter estimation [11]. Temporal activations for each of the flagged anatomical locations were determined using the current activation of the median voxel from each flagged anatomical location. For structures situated on the midline (ACC, SMA, PREC), the left and right hemispheres were combined into a single ROI, thus representing activity for the entire structure with a single current activation.

7) Quantification of Causal Relationships; EEGLab-SIFT Toolbox [6]: In order to identify causal relationships between ROI current activations computed by cLORETA, a multivariate autoregressive (MVAR) model of the data was constructed in SIFT individually for each participant, and causal connections were estimated from the MVAR model of each participant. Computation of the MVAR entailed first selecting a proper model order based on four different information criteria: the Schwarz-Bayes, Hannan-Quinn, Akaike Information Criteria, and the Final Prediction Error. The MVAR was constructed using the Vieira-Morf lattice algorithm. The whiteness of residuals, consistency, and stability of the model were tested to ensure the model was both stable and had captured a large amount of the corellational structure present in the data. The Short-time Direct Directed Transfer Function (SdDTF) was computed from the MVAR to quantify causal connections among ROIs over the course of the epoch. The SdDTF computes a spectrotemporal decomposition of causal interactions across the epoch with the added advantage of capturing only direct, rather than indirect, causal relationships between ROI's, thus preventing the appearance of phantom causal connections created by a common source. Bidirectional causality was computed for all ROI's, leading to a connectivity matrix with sources as columns and destinations as rows. The matrix is non-symmetric, as should be the case since information flow in the brain is generally non-symmetric. The diagonal represents auto-power spectra of each ROI's and may be omitted from the connectivity matrix as it does not represent any form of connectivity among the ROIs.

C. Data Processing - Deterministic Computation of Temporal Activations

A second pipeline employing deterministic computation of temporal activations was also considered as a measure of comparison to the first pipeline (section IIB). This pipeline is a form of Group-ICA that solves the problem of comparing current sources estimated through ICA by concatenating all involved datasets temporally, conducting ICA on the joint dataset, and back-projecting the ICA outcome within each subject's dataset to create a set of ICs situated in the same place, but with unique temporal activations between subjects due to different channel space data [12]. These ICs are then subjected to the same causal analysis described in step 7 of the previous section, and connectivity is computed between ICs instead of ROI's.

III. RESULTS

A. Bayesian Inference based Computation of Temporal Activations

Fig.1 shows ROIs obtained at the end of step 5. Out of the seven projected ERSP domains, the most prevalent anatomical structures were the Anterior Cingulate Cortex (ACC), the left and right orbits of the Prefrontal Cortex (PFOrbit) , the Supplementary Motor Area (SMA), the left and right Primary Visual Cortices (VIS), and the Precuneus (PREC). These locations served as the ROI's for subsequent analysis and correspond to images 3, 6, 5, 4, 1, 2, and 7 respectively at the top and left side of Fig. 4. Using the four different information criteria, the optimal MVAR order was determined to be 23

(Fig. 2), a feature consistent across all participants. The MVAR was constructed (using the Vieira-Morf lattice algorithm) with a 500 ms sliding window shifting at 30 ms increments across the epoch. The whiteness of residuals, consistency, and stability of the model are shown in Fig.3, attesting to a stable and consistent model. The Short-time Direct Directed Transfer Function (SdDTF) computed from the MVAR to quantify causal connection of ROIs over the course of the epoch led to 7x7 connectivity matrix with sources as columns and destinations as rows (Fig 4).

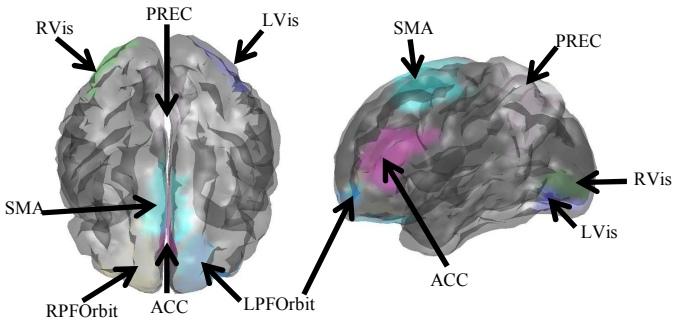

Fig. 1: Anatomical locations obtained at the end of step-5 of the first pipeline (section IIB) for a participant. These locations served as the ROI's for subsequent analysis and correspond to images 3,6,5,4,1,2, and 7 respectively at the top and left side of Fig. 4.

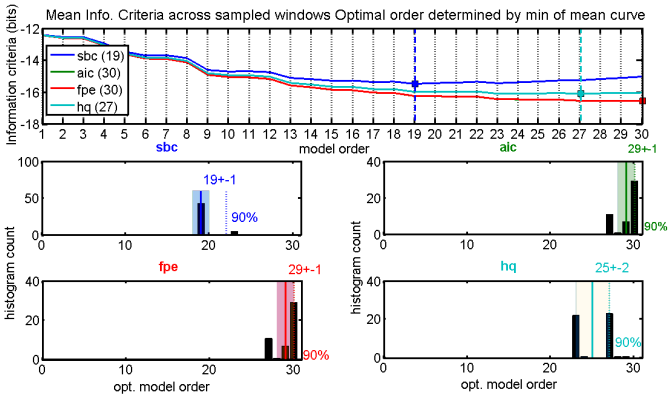

Fig. 2: Model order reported by the four information criteria. It is common for different criteria to report different model orders. The order of 23 was selected as a compromise between the order of 19 reported by sbc and the orders of 27, 30, and 30 43ported by hq, fpe, and aic respectively.

B. Deterministic Computation of Temporal Activations

The six IC clusters obtained from the group ICA are situated in regions very similar to those identified as ROIs for cLORETA (Fig.1), with the exception of the Precuneus, which did not have an analogous IC. Using the ICs, the connectivity for each participant was computed using the SdDTF and created a 6x6 causal connection matrix.

C. Analysis of Causal Relationship Matrices

Inspection of Fig. 4 reveals that strongest connection early in the epoch exists from the Right Visual Cortex (2) to the Precuneus (7), demonstrating the flow of visually relevant information around the time of the stimulus presentation. The Precuneus has causal influence on the SMA (4) over variable

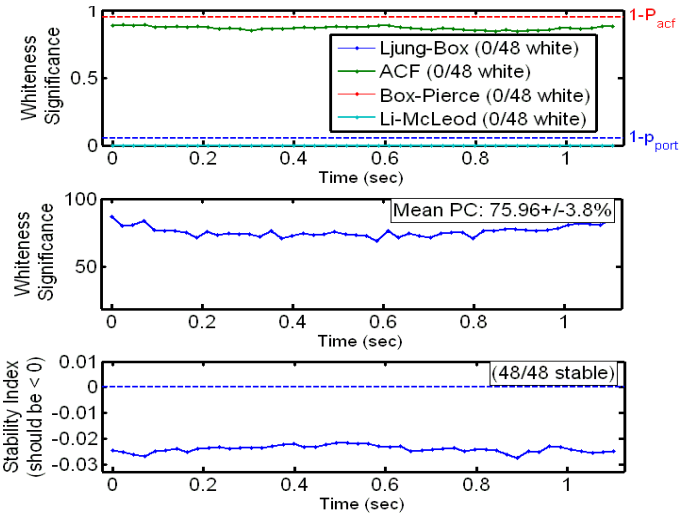

Fig. 3: Model evaluation: whiteness (top panel), consistency (middle panel), and stability (bottom panel) tests. Model residuals capture about 75% of the source activity within any given window leaving only about 25% to be explained by nonlinearities.

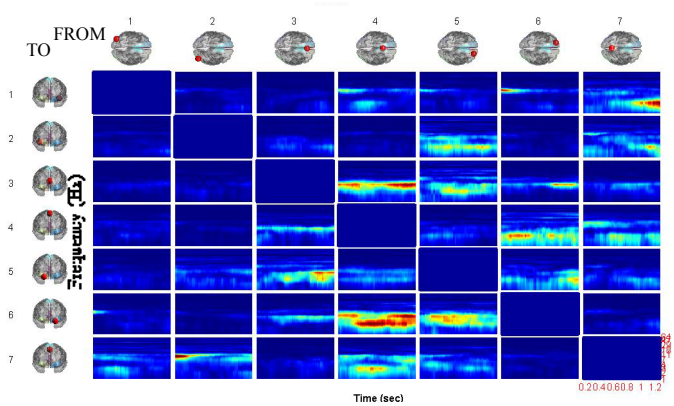

Fig. 4: Quantification of causal relationships among anatomical locations in brain ROIs specified by the position of measure projected domains during the decision process of the reward based decision making task performed by a participant. Spectrotemporal Matrix of the SdDTF (Short-time Direct Directed Transfer Function) captures time-varying connectivity between sources (locations indicated in top row images – FROM) and destinations (left indicated in left column images –TO).

frequency ranges, beginning with a high frequency narrow band toward the beginning of the epoch, and expanding in frequency to encompass lower frequency causal connection as the epoch progresses. The Precuneus also shows causal input to the ACC (3) and the Right Frontal Polar Orbit (5), as well as the Left (1) and Right (2) Visual Cortices. The ACC (3) consistently sends information over a wide frequency band to the SMA (4) and a higher, narrower band to both the Right (5) and Left (6) Frontal Polar Orbits. The Orbits exhibit a causal coupling, since both paths from Left to Right (6 to 5) and Right to Left (5 to 6) are active, as well as connections from the Right Orbit (5) to the Right Visual Cortex (2) and ACC (3), and from the Left Orbit (6) to the SMA (4). Finally, the SMA (4) provides strong feedback to the ACC (3), Left Orbit (6), and the Precuneus (7), all of which occur with a slight delay after the stimulus was presented.

Although causal interactions exist in the IC activation network, they are less extensive and less pronounced than the

interactions of Fig. 4. However, similar network topology is present, as there is visible reciprocal activity between the ACC and the analogous Right Orbit, and between the Right Orbit and Left Orbit. There is familiar feedback from the Motor Center to other ICs, but this activity is less pronounced. The Visual Cortex did not demonstrate significant outflow of information to any node in the network, a characteristic distinctly different from the active visual cortices in Fig. 4.

IV. Discussion

A framework for investigating causal relationships among brain ROIs using EEG signals was introduced. It provides algorithms for EEG data preprocessing, identification of ROIs, source localization, and causal relationship quantification. Two pipelines organized in a number of steps led to spectrotemporal causal connection matrices, used to assess causal connectivity.

Quantification of causal relationships using IC activity alone did not provide the requisite insight when it was compared to quantification of causal relationships using location specific activity provided by cLORETA. Although there are still causal interactions present in the IC activation network, they are less extensive and less pronounced than the interactions detected by LORETA. For example, in Fig. 4, the causal activity of the Precuneus, ACC, and the two Prefrontal Orbits serves as the foundation for the cortical reward-based decision making network. All four regions above send and receive information to and from each other, as well as to the captured motor (SMA) and visual (Primary Visual Cortices) areas. The Precuneus, which predominantly sent information to the motor and visual areas, is associated with visual and spatial processing, and has been shown to be involved in the planning of movements and shifts in focus between targets in motor related tasks, as was required of participants in the experiment [13]. The Prefrontal Orbits, specifically Brodmann area 11, are directly associated with risk taking tasks and decision making cognition, as evaluated in laboratory based gambling [14]. The gambling element present in the task implicates the Prefrontal Orbits in decision making between images, and the causal activity the two regions displayed over the epoch supports this implication. In terms of reward-driven decisions, the ACC has been associated both with decision making and reward processing. Of its many documented functions, it is known to process reward values, detect errors, and, in turn, affect motor responses to stimuli [15]. It is connected to the prefrontal cortex, as is functionally reflected in the LORETA causal analysis, and receives input directly from dopaminergic neurons in the midbrain, all characteristics that make it an involved member in a reward-based decision making network.

V. Concluding Remarks

The causal dynamics established by our approach demonstrate the presence of a readily detectable cortical network whose activity can be characterized when an individual is confronted with reward-based decisions. The documented connection of the cortical network to midbrain dopaminergic structures could potentially allow for inference of subcortical dopaminergic activity purely through measurement of cortical activation with EEG. This capability for non-invasive monitoring of correlates to deep-brain reward signaling using EEG holds great promise as a potential clinical diagnostic tool of neurological and neurodegenerative diseases and disorders such as ADHD, Autism, or Parkinson's disease, and the semi-synchronous BCI framework [16] we have constructed could also be used to create NFT based treatment for those diseases and disorders through behavioral reinforcement and reward.

References

[1] R. Kawagoe, Y. Takikawa, and O. Hikosaka, "Expectation of reward modulates cognitive signals in the basal ganglia," *Nat Neurosci,* vol. 1, pp. 411-6, Sep 1998.

[2] D. A. Peterson, C. Elliott, D. D. Song, S. Makeig, T. J. Sejnowski, and H. Poizner, "Probabilistic reversal learning is impaired in Parkinson's disease," *Neuroscience,* vol. 163, pp. 1092-101, Nov 10 2009.

[3] J. R. Iversen, A. Ojeda, T. Mullen, M. Plank, J. Snider, G. Cauwenberghs*, et al.*, "Causal analysis of cortical networks involved in reaching to spatial targets " in *36th Annual International Conference of the IEEE Engineering in Medicine and Biology Society (EMBC)*, Chicago, Il., USA, 2014.

[4] D. A. Peterson, D. T. Lotz, E. Halgren, T. J. Sejnowski, and H. Poizner, "Choice modulates the neural dynamics of prediction error processing during rewarded learning," *Neuroimage,* vol. 54, pp. 1385-94, Jan 15 2011.

[5] A. M. S. Delorme, "EEGLAB: an open source toolbox for analysis of single-trial EEG dynamics including independent component analysis," *Journal of Neuroscience Methods,* vol. 134, pp. 9-21, 2004.

[6] A. Delorme, T. Mullen, C. Kothe, Z. Akalin Acar, N. Bigdely-Shamlo, A. Vankov*, et al.*, "EEGLAB, SIFT, NFT, BCILAB, and ERICA: new tools for advanced EEG processing," *Comput Intell Neurosci,* vol. 2011, p. 130714, 2011.

[7] A. Gramfort, T. Papadopoulo, E. Olivi, and M. Clerc, "OpenMEEG: opensource software for quasistatic bioelectromagnetics," *Biomed Eng Online,* vol. 9, p. 45, 2010.

[8] A. J. S. Bell, T.J., "An Information-maximisation Approach to Blind Separation and Blind Deconvolution," *Neural Computation,* vol. 7.6, pp. 1004-1034, 1995.

[9] N. Bigdely-Shamlo, T. Mullen, K. Kreutz-Delgado, and S. Makeig, "Measure projection analysis: a probabilistic approach to EEG source comparison and multi-subject inference," *Neuroimage,* vol. 72, pp. 287-303, May 15 2013.

[10] R. D. Pascual-Marqui, "Discrete, 3D distributed, linear imaging methods of elec tric neuronal activity. Part 1: exact, zero error localization. ," 2007-October-17 ed, 2007

[11] N. J. Trujillo-Barreto, E. Aubert-Vazquez, and P. A. Valdes-Sosa, "Bayesian model averaging in EEG/MEG imaging," *Neuroimage,* vol. 21, pp. 1300-19, Apr 2004.

[12] T. Eichele, S. Rachakonda, B. Brakedal, R. Eikeland, and V. D. Calhoun, "EEGIFT: group independent component analysis for event-related EEG data," *Comput Intell Neurosci,* vol. 2011, p. 129365, 2011.

[13] A. E. Cavanna and M. R. Trimble, "The precuneus: a review of its functional anatomy and behavioural correlates," *Brain,* vol. 129, pp. 564-83, Mar 2006.

[14] R. D. Rogers, A. M. Owen, H. C. Middleton, E. J. Williams, J. D. Pickard, B. J. Sahakian*, et al.*, "Choosing between small, likely rewards and large, unlikely rewards activates inferior and orbital prefrontal cortex," *J Neurosci,* vol. 19, pp. 9029-38, Oct 15 1999.

[15] G. Bush, B. A. Vogt, J. Holmes, A. M. Dale, D. Greve, M. A. Jenike*, et al.*, "Dorsal anterior cingulate cortex: a role in reward-based decision making," *Proc Natl Acad Sci U S A,* vol. 99, pp. 523-8, Jan 8 2002.

[16] L. Yang, H. Leung, D. A. Peterson, T. J. Sejnowski, and H. Poizner, "Toward a semi-self-paced EEG brain computer interface: decoding initiation state from non-initiation state in dedicated time slots," *PLoS One,* vol. 9, p. e88915, 2014.